

RSC Advances



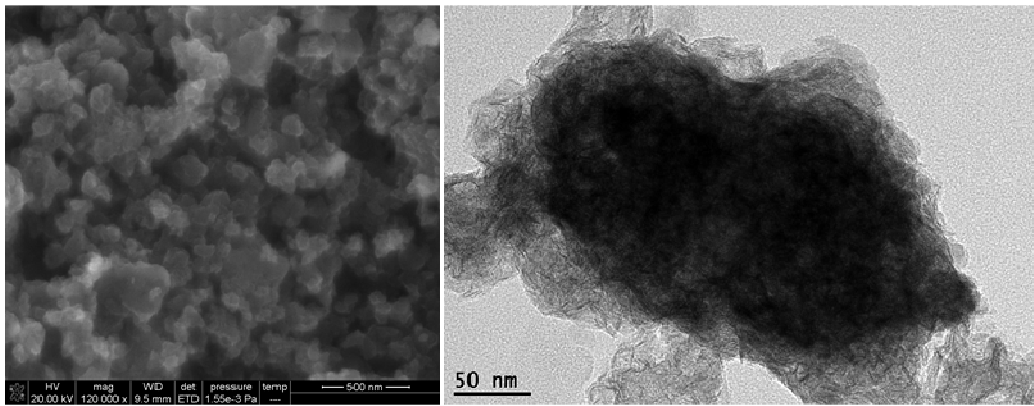
This is an *Accepted Manuscript*, which has been through the Royal Society of Chemistry peer review process and has been accepted for publication.

Accepted Manuscripts are published online shortly after acceptance, before technical editing, formatting and proof reading. Using this free service, authors can make their results available to the community, in citable form, before we publish the edited article. This *Accepted Manuscript* will be replaced by the edited, formatted and paginated article as soon as this is available.

You can find more information about *Accepted Manuscripts* in the [Information for Authors](#).

Please note that technical editing may introduce minor changes to the text and/or graphics, which may alter content. The journal's standard [Terms & Conditions](#) and the [Ethical guidelines](#) still apply. In no event shall the Royal Society of Chemistry be held responsible for any errors or omissions in this *Accepted Manuscript* or any consequences arising from the use of any information it contains.

Synthesis of novel Al/MoS₂/C composite with a facile ball milling method can improve electrochemical performance significantly as anode material for lithium-ion battery





Facile synthesis of novel Al-based composite as anode for lithium-ion batteries

Qing-Yu Li^a, Qi-Chang Pan^a, Guan-Hua Yang^a, Xi-Le Lin^a, Zhi-Xiong Yan^a, Hong-Qiang Wang^{*a,b}, You-Guo Huang^{*a}

Received 00th January 20xx,
Accepted 00th January 20xx

DOI: 10.1039/x0xx00000x

www.rsc.org/

A facile ball-milling method is developed to synthesize Al/MoS₂/C composite, which can be used for scalable industrial mass production. The composite are characterized by X-ray powder diffraction (XRD), scanning electron microscopy (SEM), transmission electron microscope (TEM), galvanostatic cycling and cyclic voltammetry. The electrochemical measurements demonstrate that the Al/MoS₂/C composite has greatly improved electrochemical performance in comparison with pure Al. After 40 cycles, the capacity retentions of Al-40wt%, Al-50wt% and Al-60wt% are 451.3 mAh g⁻¹, 419.6 mAh g⁻¹ and 378.2 mAh g⁻¹, respectively. This improved electrochemical performance may be attributed to the layer-structure MoS₂/C composite which can not only buffer the volume change but also provide stability capacity for the composite during the charge and discharge process. This suggests that Al/MoS₂/C composite has a potential possibility to be developed as an anode material for LIBs.

1. Introduction

Lithium ion batteries (LIBs), which have been regard as one of the most promising power source for electric vehicles or hybrid electric vehicles because of higher power density and longer cycle life.¹ However, graphite, the widely used as the anode materials for commercial LIBs, has a relatively low theoretical capacity and poor safety and cannot meet the demand for LIBs in the future.² In order to increase the energy density and power density for LIBs, it is necessary to develop a high-performance anode materials. Recently, transition metal oxides anode

materials and Sn-based oxide have shown significant potential for LIBs because of them possess remarkably high capacity than that of the current commercial anode materials. For example, Fe₃O₄,³⁻⁵ Fe₂O₃,^{6,7} Co₃O₄,⁸ SnO₂,⁹⁻¹¹ all of them can achieve a higher capacity than graphite, however, it suffer from a severe volume change during lithium ion insertion/extraction, which can result in a poor cycle life.

Semimetal or metal based anodes also are believed to be the most promising replaced candidates due to their high capacity and desirable working potential, such as Si,¹²⁻¹⁵ Sn,¹⁶⁻¹⁸ Sb,¹⁹ Al,²⁰⁻²² etc. the Li-Al alloy was used in the first lithium rechargeable batteries in the 1970s,²³ Al can form three kinds of alloy with lithium: AlLi, Al₂Li₃ and Al₄Li₉, all of the theoretical capacity were much higher than that of graphite. In addition, Al also has a flat and wide plateaus during the lithium ion insertion/extraction process, which is a very important factor for high-performance anode materials. Now the poor cycle life was hindered of the Al to replace the graphite, as well as known of the huge volume change is the result of that during the cycling. To overcome these problems, enormous efforts have been developed two typical approaches, one way is to synthesize nanostructured Al

^a Guangxi Key Laboratory of Low Carbon Energy Materials, School of Chemical and pharmaceutical Sciences, Guangxi Normal University, Guilin 541004, China

^b Hubei Key Laboratory for Processing and Application of Catalytic Materials, Huanggang Normal University, Huanggang 438000, China

* Hong-Qiang Wang, whq74@126.com, Fax: +86-0773-5858562

* You-Guo Huang, huangyg72@163.com

materials with various morphologies, such as Al thin film²⁴ and Al nanorod.²⁵ Other promising strategy is to construct hybrid electrodes materials. A series of Al-based composite materials such as Al-Si-graphite composite,²⁶ Al-Fe-C composite,²⁷ Co₃O₄ and SnO coated Al composite,^{28,29} or nanostructured Al_{1-x}Cu_x alloys³⁰ have been extensively reported. These composite materials though can improve the cycling performance of the Al-based composite materials in some degree, but it also not meets the high performance lithium ion batteries.

Recently, MoS₂, the typical layered transition metal sulfides with single-layer or few-layer have attracted great interest because of their excellent mechanical and electrical property.³¹ In addition, such a layered structure of MoS₂ facilitates reversible Li⁺ intercalation/extraction, which enable MoS₂ nanosheets with a high capacity up to 1000 mA h g⁻¹ for LIBs.³² Hence, MoS₂ as the substrate to form metal oxide-MoS₂ composites have been developed, such as SnO₂/MoS₂ composites³³ and Fe₃O₄/MoS₂ composites³⁴, in the composites that MoS₂ not only can effective buffer the volume change of the metal oxide but also can provide stability capacity for composites, so that can be a effective methods to prepare high-performance anode materials for LIBs. On the other hand, if the MoS₂ nanosheets are uniformly dispersed in carbon materials, which leads to enhanced electrochemical properties.³¹

In this paper, two-step synthesis of a novel Al/MoS₂/C composite is achieved by ball milling Al and MoS₂/C composite. Due to MoS₂ has excellent mechanical property, the force offered by ball milling would anchor the nanocrystalline Al particles to the MoS₂/C composite, forming a tight and stable structure. On one hand, the MoS₂/C matrix with better conductivity offers paths for fast electron transportation, increasing the reversible capacity of composites; on the other hand, the MoS₂/C matrix buffers the volume change of Al during repeated charge-discharge cycles. Therefore, the capacity and cycling performance of Al/MoS₂/C composite are greatly improved.

2. Experimental

2.1 Synthesis of MoS₂/C composite

The MoS₂/C composite was synthesis according to the literature,³¹ In a typical synthesis, 3 g of Na₂MoO₄·2H₂O and 4 g NH₂CSNH₂ were dissolved in 400 ml deionized water, and then 10 g of glucose was added into the solution. After stirring for a few minutes, the obtained clear solution was transferred into a 500 ml Teflon-lined stainless steel

autoclave and sealed tightly, heated at 240 °C for 24h. After cooling naturally, the black precipitates were collected by filter, washed with deionized water, and dried oven at 80 °C for 12 h. The MoS₂/C composite were annealed in a conventional tube furnace at 800 °C for 2 h under Ar.

2.2 Preparation of Al/MoS₂/C composite

Al and MoS₂/C composite were used as received. The Al/MoS₂/C composite were prepared by ball milling, Al and MoS₂/C composite were mixed in a 4:6 weight ratio, the weight ratio of milling balls to the powder materials was maintained as 10 to 1. Mixture was milled at a rotation speed of 350 rpm for 20 h. To prevent metal oxidation, materials handling was performed in a dry glove box with purified Ar atmosphere. Three samples, with different form Al: MoS₂/C weight ratios were prepared. Different ratios of Al to MoS₂/C were used in order to optimize the composite of electrochemical performance. Three samples, with different formal Al: MoS₂/C weight ratios, were prepared, which are listed in Table 1.

2.3 Characterization

The Phase identification of the Al and Al/MoS₂/C composite were conducted by an X-ray diffractometer (XRD, Rigaku D/max 2500) using Cu K α radiation. The microstructure of the composite and particle size distribution were investigated by scanning electron microscopy (SEM: Philips, FEI Quanta 200 FEG) and transmission electron microscopy (TEM, JEOL 2011).

2.4 Electrochemical measurements

The discharge/charge cycling performance of the samples was investigated using cell test systems (LAND BT2013A, Wuhan, China) with CR2032 coin-type cells assembled in an argon-filled glove box. The working electrodes consisted of 80 wt% of the active materials, 10 wt% conductivity agent (Super-P), and 10 wt% binder (polyvinylidene fluoride), the active material per electrode is about 0.8 mg cm⁻². Lithium foil was used both as a counter electrode and as a reference electrode in the half cells. The electrolyte was LiPF₆ (1 mol L⁻¹) in a mixture of ethylene carbonate (EC)-diethyl carbonate (DEC)-ethyl methyl carbonate (EMC) with a volume ratio EC-DEC-EMC = 1: 1: 1. Galvanostatically charge and discharge at a voltage interval of 0.05-3.0 V at a constant current of 100 mA g⁻¹. Cyclic voltammetric measurements were also carried out

on an electrochemical workstation (IM6) in a voltage range of 0.05–3.0 V at a scan rate of 0.1 mV s⁻¹.

Table 1. List of the sample with different formal Al:MoS₂/C weight ratios.

sample	Al	MoS ₂ /C
40 wt% Al	40%	60%
50 wt% Al	50%	50%
60 wt% Al	60%	40%

3. Results and discussion

Fig. 1 display the X-ray diffraction (XRD) patterns of pure Al (Fig. 1a), MoS₂/C composite (Fig. 1b) and Al/MoS₂/C composite (Fig. 1c) with different Al content. The XRD patterns showed no significant changes with increasing Al content, the four strong diffraction peak at 2θ values of 38.57°, 44.81°, 65.21° and 78.33° are found, which are attributed to the (111), (200), (220) and (311) peaks of metallic aluminum. Weak peaks of MoS₂ at 2θ = 14.2°, 33.0° and 58.9°, which are attributed to the (002), (100) and (110). However, no obvious carbon peaks appear in Fig. 1c due to the annealing temperature of 800 °C is much lower than the graphitization temperature of 3000 °C, the carbon in the Al/MoS₂/C composites should be amorphous. In the Al/MoS₂/C composite, the diffraction lines of Al and MoS₂ was seen that irrespectively and no other XRD signals was detected, indicating that MoS₂/C acts only as a dispersing medium and do not alloy with Al element to form any new phase after ball milling.

Fig. 2 illustrates the SEM photograph of pure aluminum powder and MoS₂/C composite. It was obvious that the pure aluminum powders present semi-spherical particles with an average width of about 10 μm, typical of gas-atomized metals (Fig. 2a,b). As shown in Fig 2c,d that the morphologies of the MoS₂/C composite prepared by hydrothermal and annealed that composite exhibit a sphere-like or three-dimensional architecture with a rough surface. Fig. 3 shown the SEM images of the Al/MoS₂/C composite, the morphology of the composite consisted of irregularly with nanoscale and sub-micron level. And we can not seen that obvious Al particles in the Al/MoS₂/C composite after ball milling, that because of during the ball milling process that the force induced by milling balls, and that the Al powder is broken down with reduced particle

size and uniformly dispersed in the MoS₂/C composite, so the size of about 10 μm Al powder disappear in the composite. On the other hands, it was obvious that the morphology and particles of the size of the Al/MoS₂/C composite different from those of pure Al and MoS₂/C composite after milling, indicating that the metallic Al and MoS₂/C composite have a interaction during ball milling.

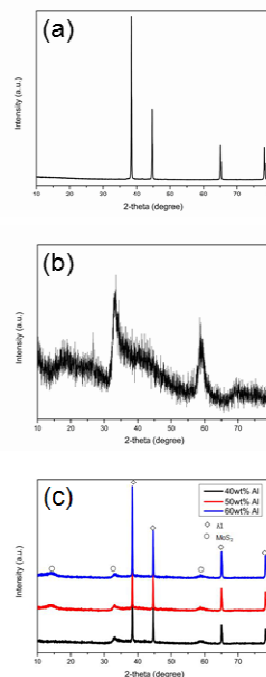


Fig. 1 XRD patterns of pure Al, MoS₂/C and Al/MoS₂/C composite: (a) pure Al, (b) MoS₂/C composite and (c) Al/MoS₂/C composite.

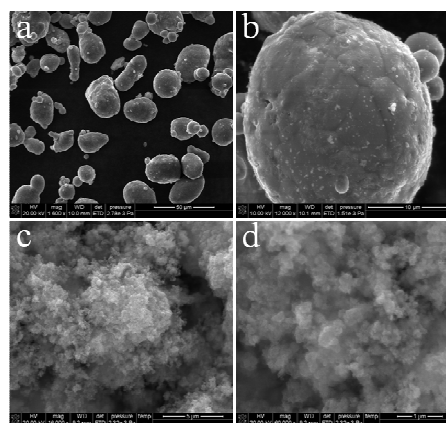


Fig. 2 SEM images of pure Al and (c, d) MoS₂/C composite.

The EDS elemental mapping in Fig. 4b-e depicts the homogeneous distribution of C, Al, Mo and S atoms in the Al/MoS₂/C composites. In addition to the four elements, the EDS also indicates the presence of trace amounts of oxygen in the composites, which could be introduced by some Al₂O₃ into products in the ball milling or prepared the Al/MoS₂/C composite process due to the Al very easy to oxidation in air. However, the Al₂O₃ not detected in the XRD, that could be because of presence of trace amounts of Al₂O₃. So the elemental mapping images clearly reveal that the Al was homogeneously dispersed in the MoS₂/C matrix.

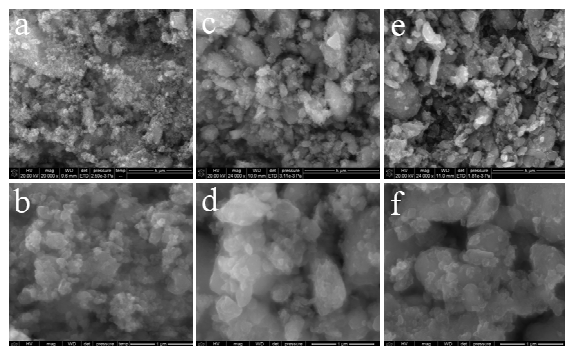


Fig. 3 SEM images of Al/MoS₂/C composite: (a, b) 40 wt.% Al, (c, d) 50 wt.% Al and (e, f) 60wt% Al.

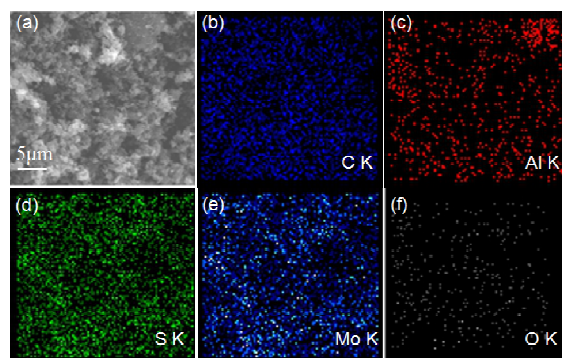


Fig. 4 EDS mappings of Al/MoS₂/C composite: (b) C, (c) Al, (d) S, (e) Mo, (f) O.

To further observed the microstructure, MoS₂/C composite and the Al/MoS₂/C composite were characterized by TEM. Fig.5 shows that the MoS₂ nanoclusters comprised of single-layer MoS₂ uniform dispersed in amorphous carbon. Moreover, Fig. 6 shows the TEM images of the Al/MoS₂/C composite. In the original MoS₂/C composite, we can clear seen that the MoS₂ dispersed in amorphous, but after the ball milling process, we can seen that some dark phase attached or embedded into the MoS₂/C matrix. According to the EDS mapping, the original Al particles reduced and

homogeneously dispersed in the MoS₂/C matrix after ball milling, so we think that the dark phase is Al. Therefore, large amounts of Al significantly reduced to nanoscale particles and some aggregate clusters of Al embedded in MoS₂/C composite in the ball milling, and the bright phase in Fig 6 c,d is MoS₂ and carbon.

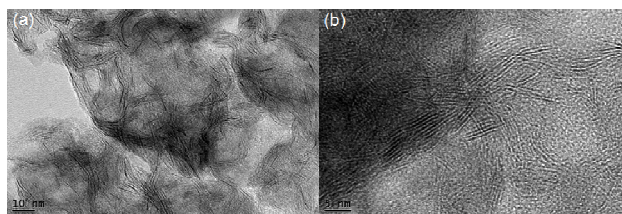


Fig. 5 TEM images of MoS₂/C composite.

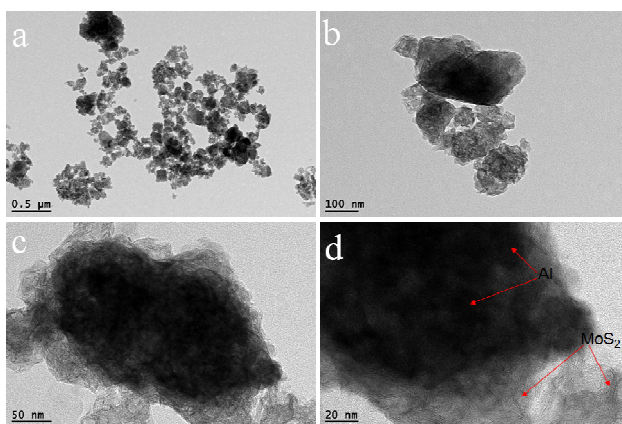


Fig. 6 TEM images of Al/MoS₂/C composite.

Fig. 7a was the first charge and discharge curves of the three Al/MoS₂/C composite samples. All the electrodes exhibited similar charge and discharge profiles, giving two charging plateau at ~ 0.5 V and at ~ 2.2 V, the plateau at about 0.5 V is indicative of the de-alloying reactions of LiAl alloy,²⁷ while the plateau about 2.2 V because of the high crystallinity of the annealed MoS₂. In addition, giving three discharging plateau at ~ 0.25 V, ~ 1.9 V and ~1.2 V, the plateau at about 0.25 V is indicative of the alloying reactions of Li with Al, and at about 1.9 V and about 1.2 V because of formation of Li_xMoS₂ and Li₂S.^{35,36}

The cyclic voltammogram of the composites electrode is shown in Fig. 7b, two oxidation peaks appeared at ~0.5 V and ~2.3 V, and three reduction peaks appeared at ~0.25 V, ~ 0.6 V and ~0.8 V during the first cycle, but the first peak at 0.6 V and 1.8 V appeared only in the initial scan and disappeared from the second and subsequent scans, implying that this reduction peaks is caused by the electrochemical reduction of electrolyte solvent for the formation of SEI film on the composites anode. Obviously,

the pair of the redox peaks at 0.2 V and 0.5 V should be attributed to the reversible alloying and dealloying reactions of lithium with aluminum, the oxidation peak at 2.3 V is attributed to the formation MoS_2 in the second and third cycle, and the reduction peak at 1.9 V is attributed to the formation Li_xMoS_2 ,³⁶ which are in accordance with the charge and discharge profiles.

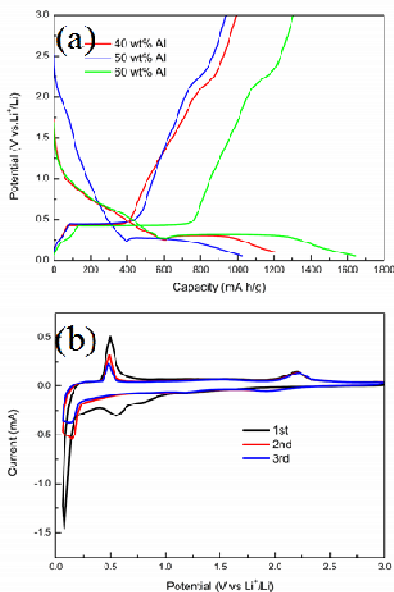


Fig. 7 (a) The first charge and discharge curves of the three Al/MoS₂/C composite at constant current of 100 mA g⁻¹. (b) Cyclic voltammograms for the Al/MoS₂/C composite at the scan rate of 0.1 mV s⁻¹.

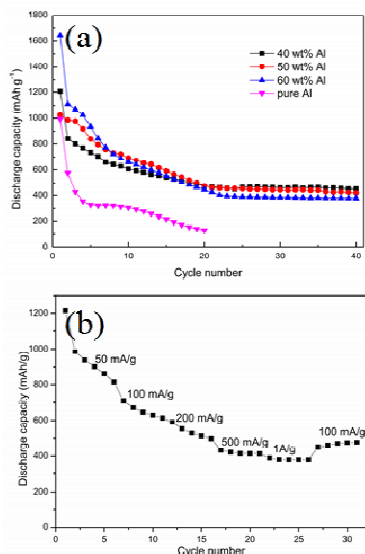


Fig. 8 Cycle performance of Al/MoS₂/C composite and pure Al electrode; (b) Rate performance of Al-40wt% Al/MoS₂/C composite

Fig. 8 shows the cycling behaviors of the Al/MoS₂/C composite and pure Al electrode under the current density of 100 mA g⁻¹ and potential range from 0.05 V - 3.0 V. The pure Al electrode delivers a diminishing discharge capacity from over 1000 mAh g⁻¹ during initial cycles to 134 mAh g⁻¹ at the 20th cycle with capacity retention of 13.4%. In the mean time, the initial discharge capacity of the three electrode was 1644.4 mAh g⁻¹, 1100.8 mAh g⁻¹ and 1206.0 mAh g⁻¹, respectively, the Al-60 wt% of the composites electrode reaches the maximum initial discharge capacity, it is show that a higher initial discharge capacity of the composites with the Al content increase. However, though the composite with the higher capacity, the capacity retention of them are poor, with the addition of more Al, the composites capacity dropped dramatically. The all of the composite of Al-40wt%, Al-50wt% and Al-60wt% deliver a reversible capacity of 451.3 mAh g⁻¹, 419.6 mAh g⁻¹ and 378.2 mAh g⁻¹ after 40 cycles, respectively. It is further proof that the Al/MoS₂/C composite exhibit much improved cycle performance and initial discharge capacity in compare to pure Al. In addition to, the cycle performance of our Al/MoS₂/C composite is more better previous reported Al-based composites for Lithium ion batteries, such as Al-Fe-C composites,²⁷ Al-Si-graphite composites,²⁶ SnO and Co₃O₄ coat Al particles composites.^{28,29} Fig. 8b shows the rate performance of the Al/MoS₂/C composite, it is observed that the discharge capacity of the Al/MoS₂/C composite were 614 mAh/g, 497 mAh/g and 413 mAh/g at the 100 mA/g, 200 mA/g and 500 mA/g current densities, respectively. Furthermore, increasing the current density of 1A/g, the discharge capacity of 379 mAh/g is still achieved. These improved electrochemical performances of the Al/MoS₂/C composites are no doubt contributed by the cooperating action of MoS₂/C composites, which not only buffers the volume change of Al, but also can provide a stability of capacity for composite electrode during the charge and discharge process. As we all known, MoS₂ has excellent mechanical property,³¹ and according to the EDS and TEM, the Al particles have been reduced to nanoparticles attached or embedded into the MoS₂/C matrix, so that the MoS₂ can buffers the volume change of Al during repeated charge-discharge cycles.

4. Conclusions

This paper describes the structural and electrochemical performance of Al/MoS₂/C composites prepared by ball milling. The experimental results revealed that the Al/MoS₂/C composites have better electrochemical

performance compared with pure Al and previous reported Al-based anode material. Particularly, the Al-40wt% composites deliver a reversible capacity of 451.3 mAh g⁻¹ after 40 cycles under current density of 100 mA g⁻¹, that showed a good cycleability. This suggests that the Al/MoS₂/C composite has a potential possibility to be developed as an anode material for Lithium ion batteries.

Acknowledgements

This research was supported by National Science Foundation of China (U1401246, 51364004, 51474077 and 21473042), Guangxi Natural Science Foundation (2013GXNSFDA019027).

Notes and references

- W. W. Lee, J. M. Lee, *J. Mater. Chem. A*, 2014, 2, 1589-1626.
- M. N. Obrovac, V. L. Chevier, *Chem. Rev.*, 2014, 23, 11444-11502.
- C. N. He, S. Wu, N. Q. Zhao, C. S. Shi, E. Z. Li and J. J. Li, *ACS Nano*, 2013, 7, 4459-4469.
- J. S. Luo, J. L. Liu, Z. Y. Zeng, C. F. Ng, L. J. Ma, H. Zhang, J. Y. Lin, Z. X. Shen and H. J. Fan, *Nano Lett.*, 2013, 13, 6136-6143.
- Y. Chen, B. H. Song, X. S. Tang, L. Lu and J. M. Xue, *Small*, 2014, 8, 1536-1543.
- H. W. Zhang, X. R. Sun, X. D. Huang and L. Zhou, *Nanoscale*, 2015, 7, 3270-3275.
- X. X. Lv, J. J. Deng, J. Wang, J. Zhong and X. H. Sun, *J. Mater. Chem. A*, 2015, 3, 5183-5188.
- L. Wang, Y. L. Zheng, X. H. Wang, S. H. Chen, H. Q. Hou and Y. H. Song, *ACS Appl. Mater. Interfaces*, 2014, 6, 7117-7125.
- Q. H. Tian, Z. X. Zhang, L. Yang and S. I. Hirano, *J. Mater. Chem. A*, 2014, 2, 12881-12887.
- B. P. Vinayan, S. Ramaprabhu, *J. Mater. Chem. A*, 2013, 1, 3865-3871.
- J. X. Wang, W. Li, F. Wang, Y. Y. Xia, Abdullah M. Asiri and D. Y. Zhao, *Nanoscale*, 2014, 6, 3217-3222.
- M. N. He, Q. Sa, G. Liu and Y. Wang, *ACS Appl. Mater. Interfaces*, 2013, 5, 11152-11158.
- L. G. Xue, G. J. Xu, Y. Li, S. L. Li, K. Fu, Q. Shi and X. W. Zhang, *ACS Appl. Mater. Interfaces*, 2013, 5, 21-25.
- R. Z. Hu, W. Sun, Y. L. Chen, M. Q. Zeng and M. Zhu, *J. Mater. Chem. A*, 2014, 2, 9118-9125.
- L. Y. Shen, Z. X. Wang and L. Q. Chen, *RSC Adv.*, 2014, 4, 15314-15318.
- J. Qin, C. N. He, N. Q. Zhao, Z. Y. Wang, C. S. Shi and J. J. Li, *ACS Nano*, 2014, 8, 1728-1738.
- X. K. Huang, S. M. Cui, J. B. Chang, Peter B. Hallac, Christopher R. Fell and J. H. Chen, *Angew. Int. Ed.*, 2014, 53, 1-5.
- J. Z. Chen, L. Yang, Z. X. Zhang, S. H. Fang and S. I. Hirano, *Chem. Commun.*, 2013, 49, 2792-2794.
- H. Bryngelsson, J. Eskhult, L. Nyholm, M. Herranen, O. Alm and K. Edstrom, *Chem. Mater.*, 2007, 19, 1170-1180.
- X. F. Lei, C. W. Wang, Z. H. Yi, Y. G. Liang and J. T. Sun, *J. Alloy. Compd.*, 2007, 429, 311-315.
- J. H. Park, C. Hudaya, A.-Y. Kim, D. K. Rhee, S. J. Yeo, W. Choi, P. J. Yoo and J. K. Lee, *Chem. Commun.*, 2014, 50, 2837-2840.
- S. P. Kuksenko, *Russ. J. Electrochem.*, 2013, 49, 67-75.
- C. J. Wen, B. A. Boukamp, R. A. Huggins, W. Weppner, *J. Electrochem. Soc.*, 1979, 126, 2258-2266.
- S. K. Sharam, M. S. Kim, D. Y. Kim and J. S. Yu, *Electrom. Acta*, 2013, 87, 872-879.
- M. Au, S. McWhorter, H. Ajo, T. Adams, Y. P. Zhao and J. Gibbs, *J. Power. Sources*, 2010, 195, 3333-3337.
- W. C. Zhou, S. Upreti and M. Stanley Whittingham, *Electrochem. Commun.*, 2011, 13, 158-161.
- Z. X. Chen, J. F. Qian, X. P. Ai, Y. L. Cao and H. X. Yang, *Electrom. Acta*, 2009, 54, 4118-4122.
- X. F. Lei, J. X. Ma, *Mater. Chem. Phys.*, 2009, 116, 383-387.
- X. F. Lei, J. F. Xiang, X. L. Ma, C. W. Wang and J. T. Sun, *J. Power. Sources*, 2007, 166, 509-513.
- C. Y. Wang, Y. S. Meng, G. Ceder and Y. Li, *J. Electrochem. Soc.*, 2008, 155, A615-A622.
- K. Chang, W. X. Chen, H. Li, F. H. Huang, Z. D. Xu, Q. B. Zhang and J. Y. Lee, *J. Mater. Chem.*, 2011, 21, 6251-6257.
- J. M. Jeong, K. G. Lee, S. J. Chang, J. W. Kim, Y. K. Han, S. J. Lee and B. G. Choi, *Nanoscale*, 2015, 7, 324-329.
- Y. Chen, J. Lu, S. Wen, L. Lu and J. M. Xue, *J. Mater. Chem. A*, 2014, 2, 17857-17866.
- Y. Chen, B. H. Song, X. S. Tang, L. Lu and J. M. Xue, *small*, 2014, 10, 1536-1543.
- K. Chang and W. X. Chen, *J. Mater. Chem.*, 2011, 21, 17175-17184.
- C. X. Lu, W. W. Liu, H. Li and B. K. Tay, *Chem. Commun.*, 2014, 50, 3338-3340.